Optimal Sharing Energy of a Complex of Houses through Energy Trading in the Internet of Energy

Chun-Cheng Lin[1,2,3], Yi-Fang Wu[1], and Wan-Yu Liu[4,5,*]

[1]*Department of Industrial Engineering and Management, National Chiao Tung University, Hsinchu 300, Taiwan*

[2]*Department of Business Administration, Asia University, Taichung 413, Taiwan*

[3]*Department of Medical Research, China Medical University Hospital, China Medical University, Taichung 404, Taiwan*

[4]*Department of Forestry, National Chung Hsing University, Taichung 402, Taiwan*

[5]*Innovation and Development Center of Sustainable Agriculture, National Chung Hsing University, Taichung 402, Taiwan*

Abstract

To increase utilization of distributed renewable energy and decrease dependence on conventional electrical grids, the Internet of energy integrates smart grids with battery energy storage systems and the Internet of things to utilize redundant energy, so that energy can be shared among users. However, few works considered sharing energy in the Internet of energy from a residential community scale. Therefore, this paper constructs a mixed-integer programming model for the optimal sharing energy of a complex of houses through the Internet of energy with an energy trading platform, by which houses with renewable energy facilities and battery energy storage systems can trade and share energy so that the

---

* Corresponding author.

E-mail address: cclin321@nctu.edu.tw (Chun-Cheng Lin), aa26717113@gmail.com (Yi-Fang Wu), wyliu@nchu.edu.tw (Wan-Yu Liu)

total profit of the whole complex of houses is maximized. This paper further solves this problem by a hybrid algorithm of harmony search and variable neighborhood search, which are good at finding optimal solutions through population search and individual search, respectively. Additionally, a solution repairing scheme is proposed to guarantee solution feasibility during the algorithm. Through simulation, this algorithm can save energy consumption of 748.17kW for one day, and shift the peak load. On the average, each house can make a profit above 70¢ for one day.

Keywords: Sharing energy, Internet of energy, energy trading, real-time price, battery energy storage

Nomenclature

Abbreviations

IoE	Internet of energy
IoT	Internet of things
BESS	Battery energy storage system
DSM	Demand side management
DER	Distributed energy resources
VPR	Virtual power plants
MIP	Mixed-integer programming
RTP	Real time price
HS	Harmony search
VNS	Variable neighborhood search
HM	Harmony memory
GA	Genetic algorithm

Parameters

n	Number of houses in the complex.
R_t	RTP for the energy supplied by the electrical grid at hour t.
P_t	The energy price for each unit of the energy traded on the energy trading platform at hour t.
$D_t^j(t)$	Energy demand of the electrical equipment of house j at hour t.
$E_{\mathrm{res}}^j(t)$	Total amount of the renewable energy harvested by house j at hour t.

$E_{\text{pv}}^{j}(t)$	Amount of the renewable energy harvested by the solar panel of house *j* at hour *t*.
$E_{\text{wind}}^{j}(t)$	Amount of the renewable energy harvested by the wind turbine of house *j* at hour *t*.
$E_{\text{storage}}^{j}(0)$	Initial energy amount of the BESS of house *j*.
$E_{\text{Maxstorage}}^{j}$	Maximal energy capacity of BESS of house *j*.
$E_{\text{platform}}(0)$	Initial energy amount on the energy trading platform.
E_{SC}	Amount of the energy charged by a BESS per hour.
Response variables	
C_{grid}	Total cost of the energy used by all houses from the electrical grid for one day.
C_{user}	Total cost of the energy purchased by all houses from the energy trading platform for one day.
R_{revenue}	Total revenue of all houses through saving and trading energy for one day.
R_{capital}	Capital value of the remaining energy stored in the BESSs of all houses at the end of one day
$E_{\text{storage}}^{j}(t)$	Energy amount stored in the BESS of house *j* at hour *t*.
$E_{\text{platform}}(t)$	Energy amount stored in the energy trading platform at hour *t*.
$\theta_{\text{gu}}^{j}(t), E_{\text{gu}}^{j}(t)$	$\theta_{\text{gu}}^{j}(t)$ is a binary variable deciding whether the electrical equipment of house *j* consumes the energy purchased from the electrical grid at hour *t*, in which 'gu' represents 'grid-equipment'. The corresponding energy amount is $E_{\text{gu}}^{j}(t)$.
$\theta_{\text{su}}^{j}(t), E_{\text{su}}^{j}(t)$	$\theta_{\text{su}}^{j}(t)$ is a binary variable deciding whether the electrical equipment of house *j* consumes the energy from the BESS at hour *t*, in which 'su' represents 'storage-equipment'. The corresponding energy amount is $E_{\text{su}}^{j}(t)$.
$\theta_{\text{pu}}^{j}(t), E_{\text{pu}}^{j}(t)$	$\theta_{\text{pu}}^{j}(t)$ is a binary variable deciding if the electrical equipment of house *j* consumes the energy purchased from the energy trading platform at hour *t*, in which 'pu' represents 'platform-equipment'. The corresponding energy amount is $E_{\text{pu}}^{j}(t)$.
$\theta_{\text{gs}}^{j}(t), E_{\text{gs}}^{j}(t)$	$\theta_{\text{gs}}^{j}(t)$ is a binary variable deciding whether the BESS of house *j* stores the energy purchased from the electrical grid at hour *t*, in which 'gs' represents 'grid-storage'. The corresponding energy amount is $E_{\text{gs}}^{j}(t)$.
$\theta_{\text{sp}}^{j}(t), E_{\text{sp}}^{j}(t)$	$\theta_{\text{sp}}^{j}(t)$ is a binary variable deciding whether the BESS of house *j* sells energy to the energy trading platform at hour *t*, in which 'sp' represents 'storage-platform'. The corresponding energy amount is $E_{\text{sp}}^{j}(t)$.

$\theta_{\mathrm{ps}}^{j}(t)$, $E_{\mathrm{ps}}^{j}(t)$	$\theta_{\mathrm{ps}}^{j}(t)$ is a binary variable deciding whether the BESS of house *j* stores the energy purchased from the energy trading platform at hour *t*, in which 'ps' represents 'platform-storage'. The corresponding energy amount is $E_{\mathrm{ps}}^{j}(t)$.
Decision variable	
$\mu_{m}^{j}(t)$	A binary variable deciding whether house *j* adopts pattern *m* in Figure 3 at hour *t*, for $m \in \{1, 2, \ldots, 21\}$.

1 Introduction

In conventional centralized electrical grids (Figure 1(a)), the power plant transmits electricity to end-users through a control center and a distribution grid, in which transmission of both information and energy is unidirectional. Generally, the conventional power plant generates energy based on the maximum energy demand in peak hours, but the unused energy in off-peak hours causes remarkable waste. With the rise of smart grids [1], smart measures have been used to monitor energy consumption of end-users, and the control center bases on the energy usage demand to set the real-time price (RTP). Based on the RTP, end-users can store energy in battery energy storage systems (BESSs) [2] for later energy use (Figure 1(b)).

Because the energy demand and the load of electrical grids vary at different times, it has been challenging for the power plant to fulfill the peak load and to adapt to the changing energy demand. With advance in technologies of the Internet of things (IoT) and increasing utilization of renewable energy, the energy management through the IoT has become increasingly essential. To control the energy infrastructure to lower the peak load, the demand side management (DSM) [4] generally adopts six methods to modify industrial, commercial, and residential users' daily and seasonal energy demand loads in peak and off-peak hours. The Internet of energy (IoE) (Figure 1(c)) integrates smart grids with BESSs and the IoT to enable intangible energy, information, and data to be public or shared [3]. Through the DSM in the IoE, utilization of distributed renewable energy can be promoted, and the dependence on electrical grids can be reduced.

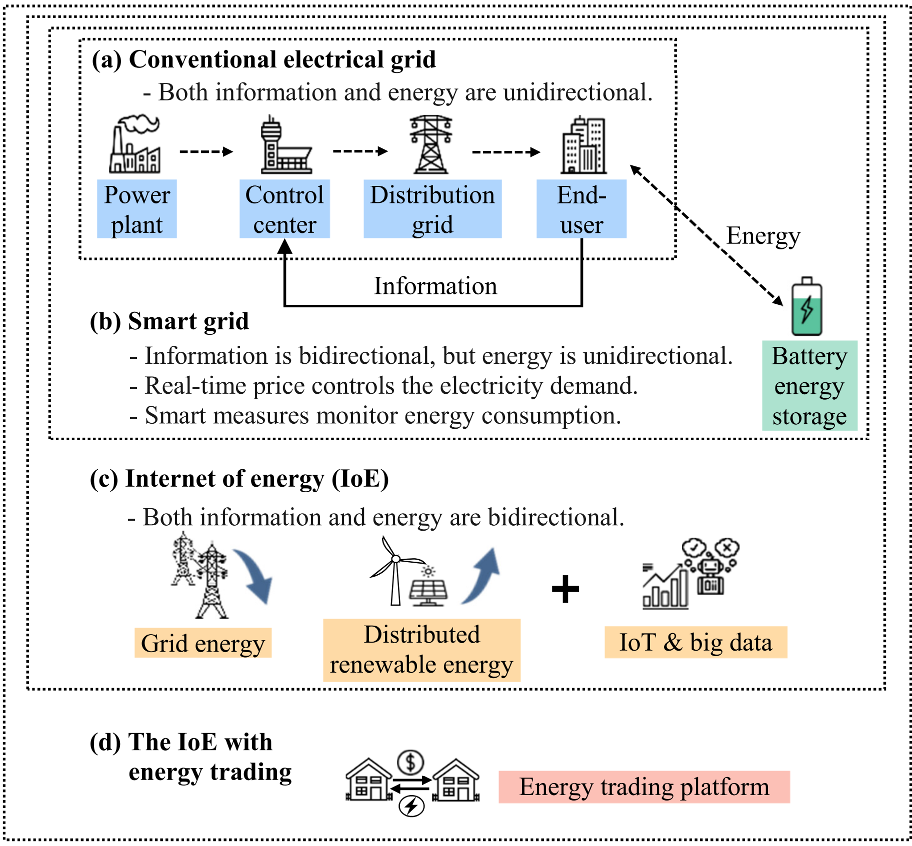

Figure 1. Classification of different energy frameworks, which form a nested structure.

To make both information and energy be bidirectional, a new trend is to introduce an energy trading platform among end-users in the IoE (Figure 1(d)), so that end-users can share energy to fully utilize redundant energy and reduce energy waste. By support of the

IoT, acquisition of full information has fostered collaborative consumption. For instance, the sharing economy allows a peer-to-peer (P2P) fashion in a community or society scale to utilize idle resources [5]. Suppliers with overabundant resources are matched with demanders with insufficient resources through a platform to efficiently provide or share goods and services, so that both of them are satisfied. Notable applications include ride sharing (e.g., Uber) and accommodation sharing (e.g., Airbnb). With loosening regulations on generating and trading energy, some countries have had practical sharing energy cases through energy trading platforms, e.g., the LO3 Energy's TransActive Grid (TAG) platform in USA, and Power Ledger's Ecochain platform in Australia. Energy can be shared through energy trading platforms, in which energy consumers are also energy prosumers, so as to maximize utilization of BESSs and renewable energy and further to adopt the DSM to alleviate the peak load problem.

Most pervious works on energy management and the IoE focused on optimal decisions of BESSs. For instance, based on the RTP, Lin *et al.* [6] regarded all end-users as a whole, and investigated their decisions on charging and discharging their BESSs to shift the peak loads in the IoE with energy trading. However, they did not provide optimal decisions, and did not consider the decision of each individual end-user. Hence, Lin *et al*. [7] considered an individual end-user with a BESS, an electric vehicle, and renewable energy facilities; and investigated this end-user's optimal charging decisions to minimize the energy usage cost through energy trading.

In light of the above, the previous works on the IoE did not consider the concept of the sharing economy for a residential community scale to maximize the total profit of operating an IoE. Consequently, this paper constructs a mixed-integer programming (MIP) model for the energy-sharing economy of a complex of houses under the IoE with energy trading. In this model, each house in the complex can harvest renewable energy through solar panels and wind turbines, store energy to its BESS, and trade energy through an energy trading platform. This paper investigates how to maximize the total profit of the complex of houses, i.e., all houses in the complex know all information, and equally share the total profit of the complex. Hence, each house makes the optimal charging/discharging decisions based on the RTP provided by the power plant and the electricity price provided by the energy trading platform. The house would buy and store energy at a low electricity price, and sell redundant energy at a high electricity price. Since MIP is NP-complete, this paper further solves this problem by a hybrid algorithm of harmony search (HS) and variable neighborhood search (VNS), which respectively have advantages in population search and individual search. Additionally, this paper proposes a scheme to repair solution infeasibility in each iteration of the algorithm. Through simulation, the performance of this algorithm is evaluated and compared with various approaches. The major contributions of this paper are as follows:

- The proposed model is the first to consider the energy-sharing economy in a residential community scale (i.e., a complex of houses, in which each house has a BESS) under the IoE with energy trading, to increase utilization of renewable energy and decrease energy waste of grids.
- This paper designs a hybrid algorithm of HS and VNS for efficiently solving the concerned problem, and proposes a repairing scheme to guarantee solution feasibility during the algorithm.

The rest of this paper is organized as follows: Section 2 gives the literature review on the relevant works. Section 3 gives the system framework, and shows the problem setting. Section 4 gives the details of the proposed HSVNS for the concerned problem. Section 5 shows the experimental results and analysis. Section 6 concludes this paper with future works.

2 Related Works

This paper investigates a *peak load shifting problem* considering *RTP* and *BESSs* in the *IoE* with *energy trading and sharing*. Hence, the works on these terms are reviewed.

2.1 Peak load shifting problem

Major strategies for peak load shaving include DSM, integration of energy storage systems (ESSs) to the grid, and integration of electric vehicles (EVs) into the grid [8]. Generally, the DSM used six methods [6] (i.e., load shifting, peak clipping, valley filling, strategic load growth, strategic conservation, and flexible load shape) to reduce the peak load demand. Among them, the most widely applicable strategies are the load shifting and peak clipping methods. Note that aside from the peak load shifting problem, DSM has also been adopted in shared electric vehicle parking market systems [9].

2.2 RTP and energy storage system (ESS)

Most works on the RTP focused on analyzing, managing, and controlling the energy price based on the demand response to the RTP; or finding optimal pricing strategies. On managing the energy price based on the RTP, Lijesen *et al.* [10] quantified the real-time dependence between spot market prices and the total peak demand. On finding optimal pricing strategies, Qian *et al.* [11] proposed a pricing control scheme that adopts the demand response management in smart grids to reduce the peak-to-average load ratio. Yoon *et al.* [12] developed a control strategy to respond to RTPs for reducing peak loads.

ESSs are used to store redundant energy. Previous works focused optimal strategies on various types of ESSs (e.g., applications of supercapacitor as external ESSs [13] in DFIG-based wind farms [14], [15], [16], [17]), and conducted management on ESSs. For instance, Abdeltawab *et al.* [18] and Hamzaoui *et al*. [19] investigated the energy management of flywheel ESSs to maintain the power output and extended the lifetime of the system. Song *et al.* [20] investigated the hybrid ESS for electric buses, and searched for the optimal supercapacitor size through energy management. Reihani *et al*. [21] proposed an optimization algorithm for charging and discharging a BESS connected to the grid with high renewables penetration. Teleke *et al*. [22] developed an optimal control strategy for using BESSs, and showed that a wind farm with a BESS is more dispatchable. To manage BESSs, Lawder *et al.* [23] adopted a management system to control how to use BESSs. Ospina *et al.* [24] managed distributed energy resources (DERs) according to the forecasted values and the RTP for energy, and further found the composition of grid, solar, and ESS power with the minimal total energy cost.

2.3 IoE

Most works on the IoE focused on transformation from smart grids to the IoE, or the applications under the IoE framework. For instance, Yi *et al.* [25] developed an EV-based energy network model that adopts EVs to transmit, distribute, and stores energy. Mahmud *et al*. [26] investigated the distributed energy management using EVs and the IoE.

Moghaddam *et al.* [27] proposed a transactive energy management system based on a fog-based IoE. Lv *et al.* [28] analyzed some models for energy security and stability in the IoE when including various distributed ESSs. Mahmud *et al.* [29] considered that all the energy prosumers in the future IoE will coordinate together to form a virtual power plants (VPRs), and surveyed the works on prosumers' management strategies for DERs and VPPs.

2.4 Energy trading and sharing

The previous works on energy trading are mainly divided into three categories: 1) proposing P2P trading applications in different scenarios (e.g., the P2P energy trading between two groups of EVs [30], and between wind energy prosumers and consumers [31]); 2) designing energy trading platforms (e.g., [32]); 3) establishing game-theoretic models on the energy trading price and finding the optimal strategies (e.g., an energy trading model based on a Nash bargaining game [33], which considers renewable energy, market price, and demand response so that all participants can fairly receive benefits).

Recently, development of the sharing economy has received much attention. The sharing economy concept has also been widely applied to energy. For instance, Zhang *et al.* [34] considered the framework in which multiple households share an ESS, and proposed a novel method of pricing and load dispatch. Cui *et al.* [35] proposed a risk aversion energy sharing model in the energy market, and established a stochastic game so as to minimize the energy cost of prosumers and the risk of the loss caused by sharing energy. Huang *et al.* [36] considered the energy sharing of ESSs in buildings and EVs; and managed their charging/discharging model that optimizes the building-cluster-level performance.

3 Problem Setting

3.1 System framework and problem description

Consider a complex of n houses in the IoE framework with an energy trading platform (Figure 2). This framework is composed as follows:

- The electrical grid sells energy to each house in the complex;
- Each house possesses multiple electrical equipment (consuming energy), a solar panel (harvesting renewable energy), a wind turbine (harvesting renewable energy), and a BESS with a different energy storage capacity (storing energy);
- An energy trading platform allows houses in the complex to trade energy between houses.

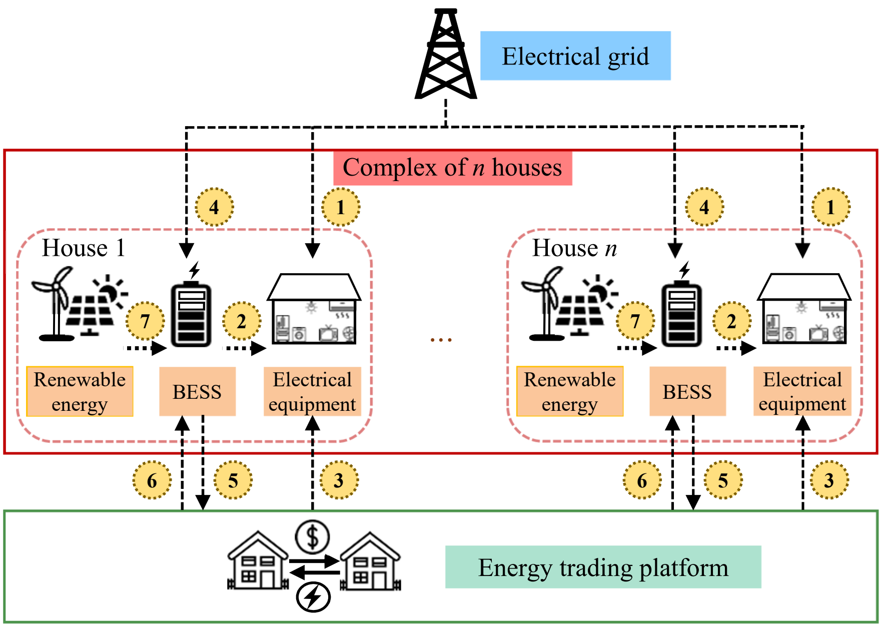

Figure 2. A complex of n houses in the IoE with an energy trading platform, in which all possible electricity flows are illustrated.

The concerned problem has the following assumptions:

1) Before the complex of houses starts one day, we have known the information of the RTP R_t for each hour t of this day, which was announced by the power plant based on the electricity demand of the previous day and the previous historical information.

2) Through the energy trading platform, each house can trade energy with other houses in the complex. The energy price P_t for each hour t adopted by the energy trading platform is set according to the RTP R_t and the energy supply and demand for this hour. The price P_t is assumed to be known.

3) Based on the historical information, the energy demand D_t^j of each house j for each hour t of this day is known.

4) No energy is consumed during transmission of the energy from the electrical grid, the energy bought from the energy trading platform, and the energy from BESSs.

5) When the renewable energy of each house is harvested, it must first be stored to the BESS of this house, and then be consumed by the electrical equipment.

6) To simplify the problem, the BESS of each house can charge and discharge energy for the same hour.

7) All houses in this complex are selfless, and pursuit maximization of the total profit of the complex.

8) The electricity flow passage can become open or close transiently according to the decisions made by the proposed algorithm at different times, and the energy loss caused by a passage change is neglected.

Note that Assumptions 1) and 2) are originated from [7]. For simplification of the problem setting, Assumptions 3)–8) are made in this paper.

With the above assumptions, the decision of each house j for each hour t is involved with the following seven electricity flows (see also the labels attached to the seven arrows in Figure 2):

1) The electrical equipment consumes the energy bought from the electrical grid at RTP R_t.
2) The electrical equipment consumes the energy stored in the BESS.
3) The electrical equipment consumes the energy bought from the energy trading platform at price P_t.
4) The BESS stores the energy bought from the electrical grid at RTP R_t.
5) The BESS sells energy to the energy trading platform at price P_t.
6) The BESS stores the energy brought from the energy trading platform at price P_t.
7) The BESS stores the renewable energy harvested by the solar panel and the wind turbine.

Given the RTP of the electrical grid and the energy price of the energy trading platform for each hour of one day, the problem concerned in this paper is to determine the electrical flows of each house in the complex for each hour to share energy through the IoE with an energy trading platform, such that the total profit of the complex of houses is maximized. By doing so, the overabundant energy can be utilized efficiently through energy trading, and the peak load problem can be alleviated.

3.2 Mathematical model of the concerned problem

This subsection constructs an MIP model for the concerned problem. First, consider the decision variables of the problem. From Figure 2, each house has seven possible electricity flows, in which the flow from the renewable energy to the BESS (labeled by 7 in Figure 2) is assumed to be a given parameter. Hence, considering whether each of six possible electricity flows is conducted, there are totally $2^6 = 64$ decision patterns. However, some of the 64 patterns are not feasible, e.g., the BESS cannot simultaneously charge and discharge energy; and the energy trading platform cannot simultaneously buy and sell energy. After removing these infeasible patterns, only 21 feasible decision patterns remain (Figure 3). The notations adopted in the problem model are given in the Nomenclature section.

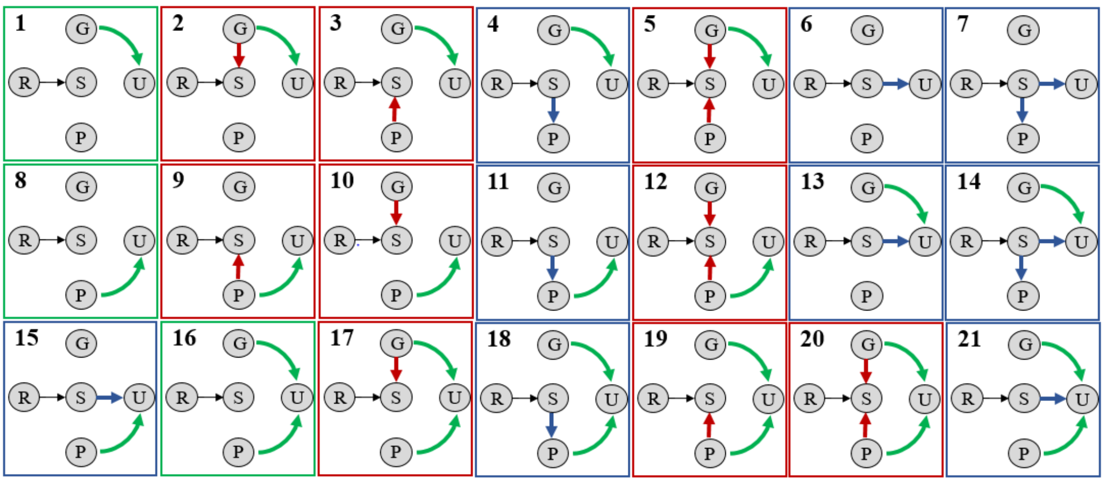

Figure 3. Illustration of 21 feasible patterns for energy flows of each house, in which 'S', 'G', 'U', 'P', and 'R' represent the BESS, electrical grid, electrical equipment, energy trading platform, and renewable energy, respectively.

The objective of the problem is to maximize the total profit of the whole complex of n houses for one day as follows:

$$\text{Maximize} \quad - C_{\text{grid}} - C_{\text{user}} + R_{\text{benefit}} + R_{\text{capital}} \tag{1}$$

where the cost C_{grid} of the energy bought by all houses from the electrical grid for 24 hours is calculated as follows:

$$C_{\text{grid}} = \sum_{j=1}^{n} \sum_{t=1}^{24} R_t \cdot \left(\theta_{\text{gu}}^j(t) \cdot E_{\text{gu}}^j(t) + \theta_{\text{gs}}^j(t) \cdot E_{\text{gs}}^j(t) \right) \tag{2}$$

The cost C_{user} of the energy bought by all houses from the energy trading platform for 24 hours is calculated as follows:

$$C_{\text{user}} = \sum_{j=1}^{n} \sum_{t=1}^{24} P_t \cdot \left(\theta_{\text{pu}}^j(t) E_{\text{pu}}^j(t) + \theta_{\text{ps}}^j(t) E_{\text{ps}}^j(t) \right) \tag{3}$$

The revenue R_{revenue} of all houses' saving and selling energy to the energy trading platform for 24 hours is calculated as follows:

$$R_{\text{revenue}} = \sum_{j=1}^{n} \sum_{t=1}^{24} \left(R_t \cdot \theta_{\text{su}}^j(t) \cdot E_{\text{su}}^j(t) + P_t \cdot \theta_{\text{sp}}^j(t) \cdot E_{\text{sp}}^j(t) \right) \tag{4}$$

The capital value R_{capital} of the remaining energy that is stored in the BESSs of all houses at the end of this day (i.e., at hour 24) is calculated as follows:

$$R_{\text{capital}} = \sum_{j=1}^{n} \left(\sum_{t=1}^{24} \left((R_t + P_t) / 48 \right) \right) \cdot E_{\text{storage}}^j(24) \tag{5}$$

Constraints of the concerned problem are given as follows. The renewable energy amount $E_{\text{res}}^j(t)$ of house j at hour t is the sum of those generated from the solar panel and the wind turbine, as expressed as follows:

$$E_{\mathrm{res}}^{j}(t)=E_{\mathrm{pv}}^{j}(t)+E_{\mathrm{wind}}^{j}(t),\forall j,t \tag{6}$$

About the price of generated electricity from the solar panel and the wind turbine, this paper supposes that the generated renewable energy can only be consumed after it is stored to the BESS (see flow 7 and then flow 2 in Figure 2), and it is further sold to the energy trading platform (see electricity flow 5 in Figure 2) at price P_t, as indicated in the above assumptions.

Constraints (7)–(9) are related to the maximal capacity. The energy amount $E_{\mathrm{storage}}^{j}(t)$ stored in the BESS of each house *j* at hour *t* has the maximal capacity $E_{\mathrm{Maxstorage}}^{j}$ as follows:

$$E_{\mathrm{storage}}^{j}(t)\le E_{\mathrm{Maxstorage}}^{j},\forall j,t \tag{7}$$

The sum of the amount of the energy sold from the BESS ($E_{\mathrm{sp}}^{j}(t)$) and the amount of the energy transmitted from the BESS to the electrical equipment ($E_{\mathrm{su}}^{j}(t)$) of each house *j* at hour *t* must be no greater than the energy amount stored in the BESS for the previous hour ($E_{\mathrm{storage}}^{j}(t-1)$) as follows:

$$\theta_{\mathrm{sp}}^{j}(t)E_{\mathrm{sp}}^{j}(t)+\theta_{\mathrm{su}}^{j}(t)E_{\mathrm{su}}^{j}(t)\le E_{\mathrm{storage}}^{j}(t-1),\forall j,t \tag{8}$$

The total energy amount stored in the BESS from the electrical grid ($E_{\mathrm{gs}}^{j}(t)$), the energy trading platform ($E_{\mathrm{ps}}^{j}(t)$), and the renewable energy ($E_{\mathrm{res}}(t)$) must be no greater than the remaining capacity of the BESS as follows:

$$\theta_{\mathrm{gs}}^{j}(t)E_{\mathrm{gs}}^{j}(t)+\theta_{\mathrm{ps}}^{j}(t)E_{\mathrm{ps}}^{j}(t)+E_{\mathrm{res}}(t)\le E_{\mathrm{Maxstorage}}^{j}-E_{\mathrm{storage}}^{j}(t-1),\forall j,t \tag{9}$$

To satisfy the energy demand of house *j*, the total sum of the energy from the electrical grid ($E_{\mathrm{gu}}^{j}(t)$), the energy storage facilities ($E_{\mathrm{su}}^{j}(t)$) and the energy trading platform ($E_{\mathrm{pu}}^{j}(t)$)

must be no less than the energy demand ($D_{\text{user}}^{j}(t)$) as follows:

$$\theta_{\text{gu}}^{j}(t)E_{\text{gu}}^{j}(t)+\theta_{\text{su}}^{j}(t)E_{\text{su}}^{j}(t)+\theta_{\text{pu}}^{j}(t)E_{\text{pu}}^{j}(t)\geq D_{\text{user}}^{j},\forall j,t \tag{10}$$

On the constraints for the energy trading platform, the energy amount in the energy trading platform for hour *t* ($E_{\text{platform}}(t)$) is equal to the energy amount in the energy trading platform for the previous hour ($E_{\text{platform}}(t-1)$) plus the amount of the energy bought from the BESSs of all houses ($\sum_{j=1}^{n}E_{\text{sp}}^{j}(t)$) deducted from the amounts of the energy sold to the electrical equipment and the BESSs of all houses ($\sum_{j=1}^{n}E_{\text{pu}}^{j}(t)+E_{\text{ps}}^{j}(t)$) as follows:

$$\begin{aligned}E_{\text{platform}}(t)=E_{\text{platform}}(t-1)+\sum_{j=1}^{n}\theta_{\text{sp}}^{j}(t)E_{\text{sp}}^{j}(t)\\-\sum_{j=1}^{n}\theta_{\text{pu}}^{j}(t)E_{\text{pu}}^{j}(t)-\sum_{j=1}^{n}\theta_{\text{ps}}^{j}(t)E_{\text{ps}}^{j}(t),\forall t\end{aligned} \tag{11}$$

The following constraint enforces that the energy sold on the energy trading platform at hour *t* must be no greater than the energy amount on the energy trading platform at hour $t-1$:

$$\sum_{j=1}^{n}\theta_{\text{pu}}^{j}(t)E_{\text{pu}}^{j}(t)+\sum_{j=1}^{n}\theta_{\text{ps}}^{j}(t)E_{\text{pu}}^{j}(t)\ \leq\ E_{\text{platform}}(t-1),\forall t \tag{12}$$

The decision variable $\mu_{m}^{j}(t)$ in this problem is a binary variable deciding whether house *j* adopts pattern *m* in Figure 3 at hour *t*, for $m\in\{1, 2, \ldots, 21\}$. The sum of these decision variables must satisfy the following constraint:

$$\sum_{m=1}^{21}\mu_{m}^{j}(t)=1,\forall j,t \tag{13}$$

$$\mu_1^j(t)\cdot\theta_{\mathrm{gu}}^j(t)=\mu_1^j(t),\forall j,t \tag{14}$$

$$\mu_1^j(t)\left(\theta_{\mathrm{gu}}^j(t)+\theta_{\mathrm{su}}^j(t)+\theta_{\mathrm{pu}}^j(t)+\theta_{\mathrm{gs}}^j(t)+\theta_{\mathrm{sp}}^j(t)+\theta_{\mathrm{ps}}^j(t)\right)=\mu_1^j(t),\forall j,t \tag{15}$$

$$\mu_2^j(t)\left(\theta_{\mathrm{gu}}^j(t)+\theta_{\mathrm{gs}}^j(t)\right)=2\mu_2^j(t),\forall j,t \tag{16}$$

$$\mu_2^j(t)\left(\theta_{\mathrm{gu}}^j(t)+\theta_{\mathrm{su}}^j(t)+\theta_{\mathrm{pu}}^j(t)+\theta_{\mathrm{gs}}^j(t)+\theta_{\mathrm{sp}}^j(t)+\theta_{\mathrm{ps}}^j(t)\right)=2\mu_2^j(t),\forall j,t \tag{17}$$

$$\mu_3^j(t)\left(\theta_{\mathrm{gu}}^j(t)+\theta_{\mathrm{ps}}^j(t)\right)=2\mu_3^j(t),\forall j,t \tag{18}$$

$$\mu_3^j(t)\left(\theta_{\mathrm{gu}}^j(t)+\theta_{\mathrm{su}}^j(t)+\theta_{\mathrm{pu}}^j(t)+\theta_{\mathrm{gs}}^j(t)+\theta_{\mathrm{sp}}^j(t)+\theta_{\mathrm{ps}}^j(t)\right)=2\mu_3^j(t),\forall j,t \tag{19}$$

$$\mu_4^j(t)\left(\theta_{\mathrm{gu}}^j(t)+\theta_{\mathrm{sp}}^j(t)\right)=2\mu_4^j(t),\forall j,t \tag{20}$$

$$\mu_4^j(t)\left(\theta_{\mathrm{gu}}^j(t)+\theta_{\mathrm{su}}^j(t)+\theta_{\mathrm{pu}}^j(t)+\theta_{\mathrm{gs}}^j(t)+\theta_{\mathrm{sp}}^j(t)+\theta_{\mathrm{ps}}^j(t)\right)=2\mu_4^j(t),\forall j,t \tag{21}$$

$$\mu_5^j(t)\left(\theta_{\mathrm{gu}}^j(t)+\theta_{\mathrm{gs}}^j(t)+\theta_{\mathrm{ps}}^j(t)\right)=3\mu_5^j(t),\forall j,t \tag{22}$$

$$\mu_5^j(t)\left(\theta_{\mathrm{gu}}^j(t)+\theta_{\mathrm{su}}^j(t)+\theta_{\mathrm{pu}}^j(t)+\theta_{\mathrm{gs}}^j(t)+\theta_{\mathrm{sp}}^j(t)+\theta_{\mathrm{ps}}^j(t)\right)=3\mu_5^j(t),\forall j,t \tag{23}$$

$$\mu_6^j(t)\cdot\theta_{\mathrm{su}}^j(t)=\mu_6^j(t),\forall j,t \tag{24}$$

$$\mu_6^j(t)\left(\theta_{\mathrm{gu}}^j(t)+\theta_{\mathrm{su}}^j(t)+\theta_{\mathrm{pu}}^j(t)+\theta_{\mathrm{gs}}^j(t)+\theta_{\mathrm{sp}}^j(t)+\theta_{\mathrm{ps}}^j(t)\right)=\mu_6^j(t),\forall j,t \tag{25}$$

$$\mu_7^j(t)\left(\theta_{\mathrm{su}}^j(t)+\theta_{\mathrm{sp}}^j(t)\right)=2\mu_7^j(t),\forall j,t \tag{26}$$

$$\mu_7^j(t)\left(\theta_{\mathrm{gu}}^j(t)+\theta_{\mathrm{su}}^j(t)+\theta_{\mathrm{pu}}^j(t)+\theta_{\mathrm{gs}}^j(t)+\theta_{\mathrm{sp}}^j(t)+\theta_{\mathrm{ps}}^j(t)\right)=2\mu_7^j(t),\forall j,t \tag{27}$$

$$\mu_8^j(t)\cdot\theta_{\mathrm{pu}}^j(t)=\mu_8^j(t),\forall j,t \tag{28}$$

$$\mu_8^j(t)\left(\theta_{\mathrm{gu}}^j(t)+\theta_{\mathrm{su}}^j(t)+\theta_{\mathrm{pu}}^j(t)+\theta_{\mathrm{gs}}^j(t)+\theta_{\mathrm{sp}}^j(t)+\theta_{\mathrm{ps}}^j(t)\right)=\mu_8^j(t),\forall j,t \tag{29}$$

$$\mu_9^j(t)\left(\theta_{\mathrm{pu}}^j(t)+\theta_{\mathrm{ps}}^j(t)\right)=2\mu_9^j(t),\forall j,t \tag{30}$$

$$\mu_9^j(t)\left(\theta_{\mathrm{gu}}^j(t)+\theta_{\mathrm{su}}^j(t)+\theta_{\mathrm{pu}}^j(t)+\theta_{\mathrm{gs}}^j(t)+\theta_{\mathrm{sp}}^j(t)+\theta_{\mathrm{ps}}^j(t)\right)=2\mu_9^j(t),\forall j,t \tag{31}$$

$$\mu_{10}^{j}(t)\left(\theta_{\mathrm{pu}}^{j}(t)+\theta_{\mathrm{gs}}^{j}(t)\right)=2\mu_{10}^{j}(t),\forall j,t \tag{32}$$

$$\mu_{10}^{j}(t)\left(\theta_{\mathrm{gu}}^{j}(t)+\theta_{\mathrm{su}}^{j}(t)+\theta_{\mathrm{pu}}^{j}(t)+\theta_{\mathrm{gs}}^{j}(t)+\theta_{\mathrm{sp}}^{j}(t)+\theta_{\mathrm{ps}}^{j}(t)\right)=2\mu_{10}^{j}(t),\forall j,t \tag{33}$$

$$\mu_{11}^{j}(t)\left(\theta_{\mathrm{pu}}^{j}(t)+\theta_{\mathrm{sp}}^{j}(t)\right)=2\mu_{11}^{j}(t),\forall j,t \tag{34}$$

$$\mu_{11}^{j}(t)\left(\theta_{\mathrm{gu}}^{j}(t)+\theta_{\mathrm{su}}^{j}(t)+\theta_{\mathrm{pu}}^{j}(t)+\theta_{\mathrm{gs}}^{j}(t)+\theta_{\mathrm{sp}}^{j}(t)+\theta_{\mathrm{ps}}^{j}(t)\right)=2\mu_{11}^{j}(t),\forall j,t \tag{35}$$

$$\mu_{12}^{j}(t)\left(\theta_{\mathrm{pu}}^{j}(t)+\theta_{\mathrm{gs}}^{j}(t)+\theta_{\mathrm{ps}}^{j}(t)\right)=3\mu_{12}^{j}(t),\forall j,t \tag{36}$$

$$\mu_{12}^{j}(t)\left(\theta_{\mathrm{gu}}^{j}(t)+\theta_{\mathrm{su}}^{j}(t)+\theta_{\mathrm{pu}}^{j}(t)+\theta_{\mathrm{gs}}^{j}(t)+\theta_{\mathrm{sp}}^{j}(t)+\theta_{\mathrm{ps}}^{j}(t)\right)=3\mu_{12}^{j}(t),\forall j,t \tag{37}$$

$$\mu_{13}^{j}(t)\left(\theta_{\mathrm{gu}}^{j}(t)+\theta_{\mathrm{su}}^{j}(t)\right)=2\mu_{13}^{j}(t),\forall j,t \tag{38}$$

$$\mu_{13}^{j}(t)\left(\theta_{\mathrm{gu}}^{j}(t)+\theta_{\mathrm{su}}^{j}(t)+\theta_{\mathrm{pu}}^{j}(t)+\theta_{\mathrm{gs}}^{j}(t)+\theta_{\mathrm{sp}}^{j}(t)+\theta_{\mathrm{ps}}^{j}(t)\right)=2\mu_{13}^{j}(t),\forall j,t \tag{39}$$

$$\mu_{14}^{j}(t)\left(\theta_{\mathrm{gu}}^{j}(t)+\theta_{\mathrm{su}}^{j}(t)+\theta_{\mathrm{sp}}^{j}(t)\right)=3\mu_{14}^{j}(t),\forall j,t \tag{40}$$

$$\mu_{14}^{j}(t)\left(\theta_{\mathrm{gu}}^{j}(t)+\theta_{\mathrm{su}}^{j}(t)+\theta_{\mathrm{pu}}^{j}(t)+\theta_{\mathrm{gs}}^{j}(t)+\theta_{\mathrm{sp}}^{j}(t)+\theta_{\mathrm{ps}}^{j}(t)\right)=3\mu_{14}^{j}(t),\forall j,t \tag{41}$$

$$\mu_{15}^{j}(t)\left(\theta_{\mathrm{su}}^{j}(t)+\theta_{\mathrm{pu}}^{j}(t)\right)=2\mu_{15}^{j}(t),\forall j,t \tag{42}$$

$$\mu_{15}^{j}(t)\left(\theta_{\mathrm{gu}}^{j}(t)+\theta_{\mathrm{su}}^{j}(t)+\theta_{\mathrm{pu}}^{j}(t)+\theta_{\mathrm{gs}}^{j}(t)+\theta_{\mathrm{sp}}^{j}(t)+\theta_{\mathrm{ps}}^{j}(t)\right)=2\mu_{15}^{j}(t),\forall j,t \tag{43}$$

$$\mu_{16}^{j}(t)\left(\theta_{\mathrm{gu}}^{j}(t)+\theta_{\mathrm{pu}}^{j}(t)\right)=2\mu_{16}^{j}(t),\forall j,t \tag{44}$$

$$\mu_{16}^{j}(t)\left(\theta_{\mathrm{gu}}^{j}(t)+\theta_{\mathrm{su}}^{j}(t)+\theta_{\mathrm{pu}}^{j}(t)+\theta_{\mathrm{gs}}^{j}(t)+\theta_{\mathrm{sp}}^{j}(t)+\theta_{\mathrm{ps}}^{j}(t)\right)=2\mu_{16}^{j}(t),\forall j,t \tag{45}$$

$$\mu_{17}^{j}(t)\left(\theta_{\mathrm{gu}}^{j}(t)+\theta_{\mathrm{pu}}^{j}(t)+\theta_{\mathrm{gs}}^{j}(t)\right)=3\mu_{17}^{j}(t),\forall j,t \tag{46}$$

$$\mu_{17}^{j}(t)\left(\theta_{\mathrm{gu}}^{j}(t)+\theta_{\mathrm{su}}^{j}(t)+\theta_{\mathrm{pu}}^{j}(t)+\theta_{\mathrm{gs}}^{j}(t)+\theta_{\mathrm{sp}}^{j}(t)+\theta_{\mathrm{ps}}^{j}(t)\right)=3\mu_{17}^{j}(t),\forall j,t \tag{47}$$

$$\mu_{18}^{j}(t)\left(\theta_{\mathrm{gu}}^{j}(t)+\theta_{\mathrm{pu}}^{j}(t)+\theta_{\mathrm{sp}}^{j}(t)\right)=3\mu_{18}^{j}(t),\forall j,t \tag{48}$$

$$\mu_{18}^{j}(t)\left(\theta_{\mathrm{gu}}^{j}(t)+\theta_{\mathrm{su}}^{j}(t)+\theta_{\mathrm{pu}}^{j}(t)+\theta_{\mathrm{gs}}^{j}(t)+\theta_{\mathrm{sp}}^{j}(t)+\theta_{\mathrm{ps}}^{j}(t)\right)=3\mu_{18}^{j}(t),\forall j,t \tag{49}$$

$$\mu_{19}^{j}(t)\left(\theta_{\mathrm{gu}}^{j}(t)+\theta_{\mathrm{pu}}^{j}(t)+\theta_{\mathrm{ps}}^{j}(t)\right)=3\mu_{19}^{j}(t),\forall j,t \tag{50}$$

$$\mu_{19}^{j}(t)\left(\theta_{\mathrm{gu}}^{j}(t)+\theta_{\mathrm{su}}^{j}(t)+\theta_{\mathrm{pu}}^{j}(t)+\theta_{\mathrm{gs}}^{j}(t)+\theta_{\mathrm{sp}}^{j}(t)+\theta_{\mathrm{ps}}^{j}(t)\right)=3\mu_{19}^{j}(t),\forall j,t \tag{51}$$

$$\mu_{20}^{j}(t)\left(\theta_{\mathrm{gu}}^{j}(t)+\theta_{\mathrm{pu}}^{j}(t)+\theta_{\mathrm{gs}}^{j}(t)+\theta_{\mathrm{ps}}^{j}(t)\right)=4\mu_{20}^{j}(t),\forall j,t \tag{52}$$

$$\mu_{20}^{j}(t)\left(\theta_{\mathrm{gu}}^{j}(t)+\theta_{\mathrm{su}}^{j}(t)+\theta_{\mathrm{pu}}^{j}(t)+\theta_{\mathrm{gs}}^{j}(t)+\theta_{\mathrm{sp}}^{j}(t)+\theta_{\mathrm{ps}}^{j}(t)\right)=4\mu_{20}^{j}(t),\forall j,t \tag{53}$$

$$\mu_{21}^{j}(t)\left(\theta_{\mathrm{gu}}^{j}(t)+\theta_{\mathrm{su}}^{j}(t)+\theta_{\mathrm{pu}}^{j}(t)\right)=3\mu_{21}^{j}(t),\forall j,t \tag{54}$$

$$\mu_{21}^{j}(t)\left(\theta_{\mathrm{gu}}^{j}(t)+\theta_{\mathrm{su}}^{j}(t)+\theta_{\mathrm{pu}}^{j}(t)+\theta_{\mathrm{gs}}^{j}(t)+\theta_{\mathrm{sp}}^{j}(t)+\theta_{\mathrm{ps}}^{j}(t)\right)=3\mu_{21}^{j}(t),\forall j,t \tag{55}$$

The above decision variables only make binary decisions of energy flows, but do not determine the energy amount of each flow. Hence, the following constraints determine the corresponding energy amounts:

$$E_{\mathrm{su}}^{j}(t)\theta_{\mathrm{su}}^{j}(t)=\min\left(D_{\mathrm{user}}^{j}(t),E_{\mathrm{storage}}^{j}(t-1)\right) \tag{56}$$

$$E_{\mathrm{pu}}^{j}(t)\theta_{\mathrm{pu}}^{j}(t)=D_{\mathrm{user}}^{j}(t)-E_{\mathrm{su}}^{j}(t)\theta_{\mathrm{su}}^{j}(t) \tag{57}$$

$$E_{\mathrm{gu}}^{j}(t)\theta_{\mathrm{gu}}^{j}(t)=D_{\mathrm{user}}^{j}(t)-E_{\mathrm{su}}^{j}(t)\theta_{\mathrm{su}}^{j}(t)-E_{\mathrm{pu}}^{j}(t)\theta_{\mathrm{pu}}^{j}(t) \tag{58}$$

$$E_{\mathrm{gs}}^{j}(t)\theta_{\mathrm{gs}}^{j}(t)=E_{\mathrm{SC}} \tag{59}$$

$$E_{\mathrm{sp}}^{j}(t)\theta_{\mathrm{sp}}^{j}(t)=E_{\mathrm{storage}}^{j}(t-1)-E_{\mathrm{su}}^{j}(t)\theta_{\mathrm{su}}^{j}(t) \tag{60}$$

$$E_{\mathrm{ps}}^{j}(t)\theta_{\mathrm{ps}}^{j}(t)=E_{\mathrm{SC}} \tag{61}$$

The constraints of all binary variables are as follows:

$$\theta_{\mathrm{gu}}^{j}(t),\theta_{\mathrm{su}}^{j}(t),\theta_{\mathrm{pu}}^{j}(t),\theta_{\mathrm{gs}}^{j}(t),\theta_{\mathrm{ps}}^{j}(t),\theta_{\mathrm{sp}}^{j}(t)\in\{0,1\},\forall j,t \tag{62}$$

$$\mu_{m}^{j}(t)\in\{0,1\},\forall j,t,m \tag{63}$$

4 The Proposed Algorithm

The idea behind the HS [37], [38] is to search for the optimal solution of the concerned problem through simulating a process of improvisation of multiple musicians to find the perfect harmony (i.e., candidate solution) consisting of multiple notes (i.e., decision variables), and keeping the best harmonies found so far in a harmony memory (HM for short). The HS has been adopted for solving various optimization problems, e.g., the combined economic emission dispatch problem of microgrids [39] and short-term hydrothermal scheduling [40]. On the other hand, the idea behind the VNS [42], [41] is to iteratively apply a number of neighborhood searching methods until no further improved solutions are found, in which each neighborhood searching method searches for an improved solution in the neighborhood of the current solution. This paper proposes a novel hybrid algorithm integrating HS and VNS (HSVNS for short) for solving the concerned problem. The proposed HSVNS is given in Algorithm 1.

Algorithm 1 HSVNS

Initialize a harmony memory HM consisting of *hms* harmonies by Algorithm 4
Evaluate the fitness of each harmony in the HM by Algorithm 2
while the maximal iteration number η_1 is not achieved or the HM has not been updated for a given number of iterations **do**
    Use the VNS shaking procedure to generate a new harmony X_{new} by Algorithm 7
    while the maximal iteration number η_2 is not achieved **do**
        for k = 1 to 3 **do**
            Use the VNS neighborhood structure N_k to generate a harmony X' based on harmony X_{new} by Algorithm 9, in which the three structures are based on the memory consideration, pitch adjustment, and random operators inspired from the HS, respectively.
            Replace harmony X_{new} by harmony X' if harmony X' is better
        next for
    end while
    Replace the worst harmony X_{worst} in the HM by harmony X_{new} if X_{new} is better
end while
Output the solution corresponding to the best harmony X_{best} in the HM

4.1 Solution representation and fitness evaluation

As mentioned in the last section, only 21 feasible decision patterns for energy flows of each house remain (Figure 3). Therefore, considering a complex of n houses for 24 hours, a harmony (i.e., candidate solution) X of the proposed algorithm is encoded as a two-dimensional matrix as follows: $X = [M_{jt}]_{n\times 24}$, where for $j \in \{1, 2, \ldots, n\}$ and $t \in \{1, 2, \ldots, 24\}$, note $M_{jt} \in \{1, 2, \ldots, 21\}$ denotes the index of the pattern that house j employs at hour t. That is, a harmony consists of $n \times 24$ notes. The fitness of harmony X is denoted by $f(X)$, which is set as the objective function in (1) in this paper. Given a harmony $X = [M_{jt}]_{n\times 24}$, the fitness $f(X)$ is evaluated in Algorithm 2, in which Line 1 of Algorithm 2 calls Algorithm 3 to compute all the related energy amounts.

Algorithm 2 EVALUATE FITNESS

Input: A harmony $X = [M_{jt}]_{n\times 24}$
Output: Fitness $f(X)$ of harmony X

1: **for** t =1 to 24 **do**
2:     **for** j =1 to n **do**
3:         Compute the energy amount of each flow of house j at hour t by Algorithm 3
4:     **next for**
5: **next for**
6: Let $C_{\text{grid}} = C_{\text{user}} = R_{\text{revenue}} = R_{\text{capital}} = 0$
7: **for** j =1 to n **do**
8:     **for** t =1 to 24 **do**
9:         $C_{\text{grid}} = C_{\text{grid}} + R(t) \cdot \left(E_{\text{gu}}^{j}(t) + E_{\text{gs}}^{j}(t)\right)$
10:         $C_{\text{user}} = C_{\text{user}} + P(t) \cdot \left(E_{\text{pu}}^{j}(t) + E_{\text{ps}}^{j}(t)\right)$
11:         $R_{\text{revenue}} = R_{\text{revenue}} + R(t) \cdot E_{\text{su}}^{j}(t) + P(t) \cdot E_{\text{sp}}^{j}(t)$
12:     **next for**
13:     $R_{\text{capital}} = R_{\text{capital}} + \left(\sum_{t=0}^{24} (R_t + P_t) / 48\right) \cdot E_{\text{storage}}^{j}(24)$
14: **next for**
15: $f(X) = -C_{\text{grid}} - C_{\text{user}} + R_{\text{revenue}} + R_{\text{capital}}$

Algorithm 3 COMPUTE ALL ENERGY AMOUNTS

Input: A note M_{jt}

Output: Energy amounts $E^{j}_{\text{su}}(t)$, $E^{j}_{\text{pu}}(t)$, $E^{j}_{\text{gu}}(t)$, $E^{j}_{\text{gs}}(t)$, $E^{j}_{\text{sp}}(t)$, $E^{j}_{\text{ps}}(t)$, and $E^{j}_{\text{storge}}(t)$ of house j at hour t

1: Obtain a pattern in Figure 3 corresponding to M_{jt}, which further determines all binary decision variables $\mu^{j}_{\text{su}}(t)$, $\mu^{j}_{\text{pu}}(t)$, $\mu^{j}_{\text{gu}}(t)$, $\mu^{j}_{\text{gs}}(t)$, $\mu^{j}_{\text{sp}}(t)$, and $\mu^{j}_{\text{ps}}(t)$ of house j at hour t

2: Based on the above results to compute $E^{j}_{\text{su}}(t)$, $E^{j}_{\text{pu}}(t)$, $E^{j}_{\text{gu}}(t)$, $E^{j}_{\text{gs}}(t)$, $E^{j}_{\text{sp}}(t)$, and $E^{j}_{\text{ps}}(t)$ by (56)–(61)

3: $E^{j}_{\text{storge}}(t) = \min(E^{j}_{\text{storge}}(t-1) + E^{j}_{\text{res}}(t) + E^{j}_{\text{gs}}(t) + E^{j}_{\text{ps}}(t) - E^{j}_{\text{sp}}(t), E^{j}_{\text{Maxstorge}})$

4.2 Solution initialization and solution repairing

The 21 feasible decision patterns of energy flows in Figure 2 are divided into three pattern classes:

- The decision patterns where the BESS charges energy: The set of these IDs is denoted by $C_{\text{charge}} = \{2, 3, 5, 9, 10, 12, 17, 19, 20\}$;
- The decision patterns where the BESS discharges energy: The set of these IDs is denoted by $C_{\text{discharge}} = \{4, 6, 7, 11, 13, 14, 15, 18, 21\}$;
- The other decision patterns, i.e., the BESS does not charge nor discharge energy: The set of these IDs is denoted by $C_{\text{maintain}} = \{1, 8, 16\}$.

The initialization of the HM in the HSVNS is given in Algorithm 4, in which Line 12 (resp., Line 15) calls Algorithm 5 (resp., Algorithm 6) to check whether a note (resp., a harmony) is infeasible, and repair it if necessary.

Algorithm 4 INITIALIZE THE HM

Output: A HM of *hms* harmonies, in which the *s*th harmony is denoted by $X_s = [M_{jt}^s]_{n \times 24}$

for s = 1 to *hms* **do**
  for t = 1 to 24 **do**
    for j = 1 to n **do**
      if $E_{\text{storage}}^j(0) = E_{\text{Maxstorage}}^j$ **then**
        M_{jt}^s = a random number from $C_{\text{discharge}} \cup C_{\text{maintain}}$
      else if $E_{\text{storage}}^j(0) > 0$ **then**
        M_{jt}^s = a random number from $\{1, 2, \ldots, 5\} \cup \{8, 9, \ldots, 21\}$ (i.e., all the patterns except for patterns 6 and 7)
      else
        M_{jt}^s = a random number from $C_{\text{charge}} \cup C_{\text{maintain}}$
      end if
      Compute the energy amount of each flow of house j at hour t by Algorithm 3
      Call Algorithm 5 to repair M_{jt}^s
    next for
    Calculate $E_{\text{platform}}(t)$ based on (11)
    Call Algorithm 6 to repair all the notes so far
  next for
  Evaluate the fitness $f(X_s)$ of harmony X_s by Algorithm 2
end for

Algorithm 5 REPAIR A NOTE

Input: A note M_{jt} when all the notes of house j when all the notes of house j before hour t have been known to be feasible

Required: Note M_{jt} must be feasible in the harmony X_s

if $E_{\text{su}}^j(t) + E_{\text{sp}}^j(t) > E_{\text{storage}}^j(t-1)$ **then**
  Let M_{jt}^s = 1, and call Algorithm 3 to compute the energy amount of each flow of house j at hour t
end if

Algorithm 6 REPAIR A COLUMN

Input: All the notes of all houses at hour t when all the notes of all houses at before hour t have been known to be feasible

Required: All the above noes must be feasible in the harmony X_s

if $\sum_{j=1}^{n} E_{\text{pu}}^{j}(t) + \sum_{j=1}^{n} E_{\text{ps}}^{j}(t) > E_{\text{platform}}(t-1)$ **then**

  Let S be the set of IDs of the users that employ patterns related to the energy trading platform (i.e., 3, 5, 8, 9, 10, 11, 12, 15, 16, 17, 18, 19, 20, 21) at hour t

  while $S \neq \varnothing$ **do**

    Randomly select a user ID j from S, and let S = S \ {j}

    Let M_{jt}^{s} = 1, and call Algorithm 3 to compute the energy amount of each flow of house j at hour t

    Calculate $E_{\text{platform}}(t)$ based on (11)

    If $\sum_{j=1}^{n} E_{\text{pu}}^{j}(t) + \sum_{j=1}^{n} E_{\text{ps}}^{j}(t) \le E_{\text{platform}}(t-1)$, then break the while loop

  end while

end if

4.3 VNS shaking and HS operators in the HSVNS

The VNS shaking is given in Algorithm 7 (in which Algorithm 8 is used to partially repair the harmony), and the VNS neighborhood changing based on HS is given in Algorithm 9, which also requires the repairing scheme in Algorithm 8.

Algorithm 7 SHAKE

Input: A HM with *hms* harmonies

Output: A harmony X_{new}

Randomly select a harmony $X_s = [M_{jt}^{s}]_{n\times 24}$ from the HM, in which $s \in \{1, 2, \ldots, hms\}$

Randomly select a hour t from {1, 2, …, 24}

Randomly select a user j from {1, 2, …, n}

Randomly select a user k with the same pattern class with user j from {1, 2, …, n}

Swap the value of M_{jt}^{s} with that of M_{kt}^{s} in harmony X_s

Call Algorithm 5 to repair M_{jt}^{s} and M_{kt}^{s}

Call Algorithm 8 to repair all the notes after hour t in X_s

Evaluate fitness of harmony X_s, and output harmony X_s as X_{new}

Algorithm 8 REPAIR NOTES AFTER HOUR t

for $\tau = t + 1$ to 24 **do**
  for j =1 to n **do**
    Call Algorithm 5 to repair $M_{j\tau}$
  end for
  Call Algorithm 6 to repair all notes of house j at all hours
next for

Algorithm 9 NEIGHBORHOOD CHANGE

Input: A harmony X_{new} and the index k of the neighborhood structure
Output: A harmony X'

Let X' be a copy of harmony X_{new}
Randomly choose a harmony index s from $\{1, 2, \ldots, hms\}$
Randomly choose a user ID j from $\{1, 2, \ldots, n\}$
Replace all the notes of house j at all hours in harmony X' by the corresponding notes in harmony X_s
Call Algorithm 8 to repair all the notes after hour 0 in X'
if $k > 1$ **then**
  if a random value from [0, 1] < 0.5 **then**
    τ_1 is assigned with a random hour index from $\{1, 2, \ldots, 24\}$
    Randomly select a hour index τ_2 so that the notes of house j at hours τ_1 and τ_2 are of the same pattern class in harmony X'
  else
    Randomly select one pattern class C from $\{C_{\text{charge}}, C_{\text{discharge}}, C_{\text{maintain}}\}$
    Randomly select two hour indices τ_1 and τ_2 so that the notes of house j at hours τ_1 and τ_2 are of the pattern class C in harmony X'
  end if
  Swap the values of the two notes of house j at hours τ_1 and τ_2 in harmony X'
  Call Algorithm 8 to repair all the notes after hour $\min(\tau_1, \tau_2) - 1$ in X'
  if $k = 3$ **then**
    Randomly select a hour index t from $\{1, 2, \ldots, 24\}$
    The note of house j at hour t is assigned with a random pattern ID from $\{1, 2, \ldots, 21\}$ in harmony X'
    Call Algorithm 8 to repair all the notes after hour $t - 1$ in X'
  end if
end if

5 Implementation and Experimental Results

The experimental parameters are set as follows. The number of houses in a complex (n) is ranged in [5, 150] (n = 5 by default). From [43], E_{SC} = 5 (kW), based on which the following parameters are set accordingly: $E_{\text{platform}}(0) = 150$ (kW); and for each j, $E^j_{\text{Maxstorage}}$ = 50 (kW), and $E^j_{\text{storage}}(0)$ is set randomly from {0, 10, 20, 30, 40, 50} (kW). Since houses in a complex are located in the same area, the energy harvested by the solar panel and the wind turbine (i.e., $E^j_{pv}(t)$ and $E^j_{\text{wind}}(t)$) of each house is supposed to be the same at each hour (Figure 4), referred to the data from [44]. Figure 5 shows the RTP R_t (from the RTP on Feb. 19, 2019 in [45]) and the energy price P_t of the energy trading platform for 24 hours through conducting simulation on the RTP data in [44].

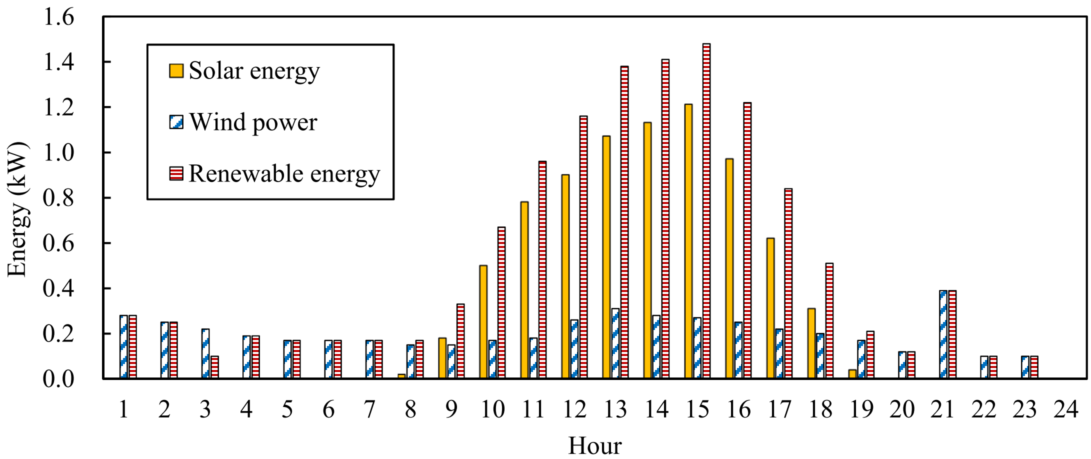

Figure 4. The average amount of the renewable energy harvested by the solar panel and the wind turbine of each house for 24 hours.

Referred to [46], there are four kinds of hourly energy demand of electrical equipment based on different users: office workers, students, the elder, and night workers (Figure 6). Then, this paper supposes the composition of the above four types of users in each house of the complex (e.g., Table 1 for five houses), and further simulates the hourly energy demand of the electrical equipment of each house based on its user composition (e.g., Figure 7).

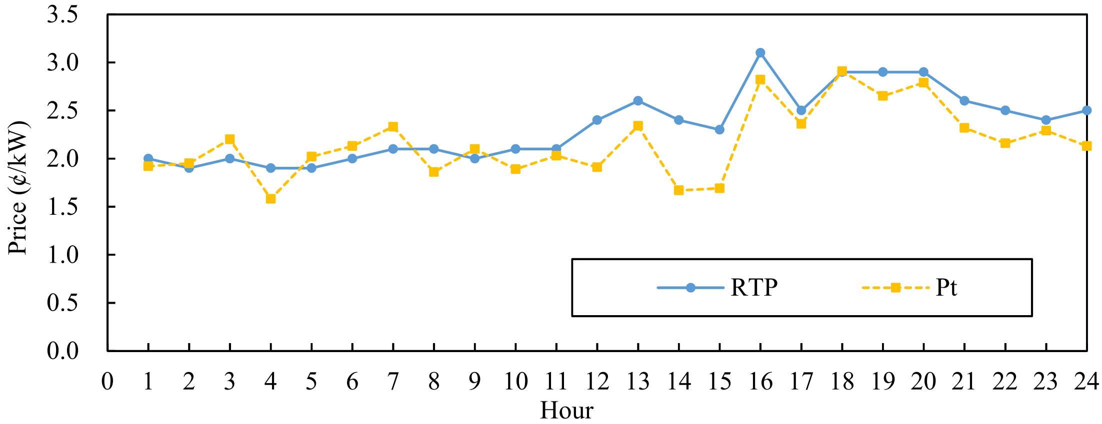

Figure 5. The RTP and the energy price P_t of the energy trading platform.

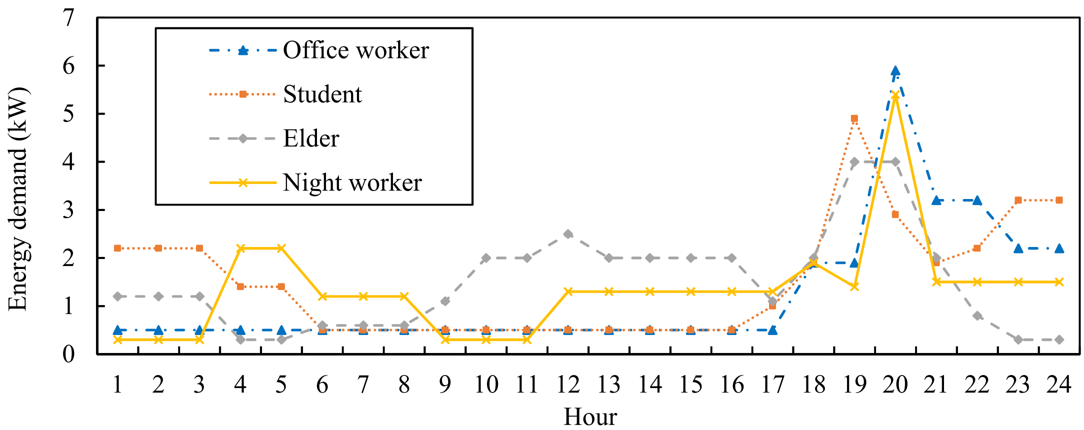

Figure 6. The hourly energy demand of the electrical equipment of four kinds of users for one day.

Table 1. Composition of four types of users in five houses.

House ID	Number of house members	Office worker	Student	Elder	Night worker
1	2	2	0	0	0
2	2	1	0	1	0
3	2	0	0	1	1
4	3	0	2	0	1
5	3	1	0	1	1

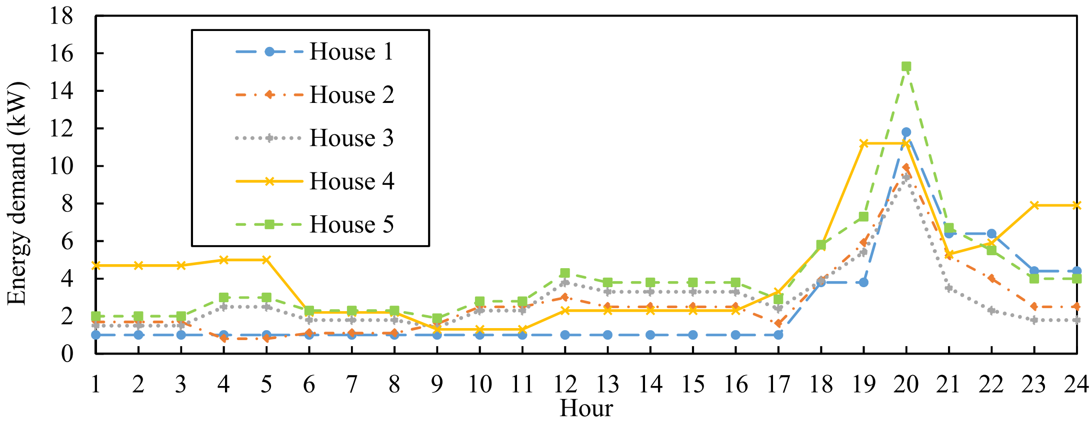

Figure 7. The hourly energy demand of the electrical equipment of five houses for one day, in which each house has different user composition.

After a lot of trials, unless stated otherwise, the parameters used in the HSVNS are set as follows: η_1 = 10000, η_2 = 100, and *hms* = 20. All the experiments are executed on a personal computer with an Intel Core^{TM} i5-6400 CPU @2.70GHz and 8GB memory.

5.1 Convergence analysis

For experimental comparison, the proposed HSVNS is compared with the classical HS and VNS, because the HSVNS is a hybrid algorithm of them. In addition, it is also compared with the genetic algorithm (GA), because the GA is one of the most notable population-based metaheuristic algorithms. In all experimental comparison in this subsection, the four algorithms are analyzed under their best parameter settings after a lot of experimental trials. On average CPU time, each iteration of the HSVNS, HS, VNS, and GA takes about 3.27ms, 18.63μs, 2.00ms, and 0.24ms, respectively. The convergence analysis of the four algorithms is shown in Figure 8. From Figure 8, the proposed HSVNS obtains the best result, and has the best convergence efficiency.

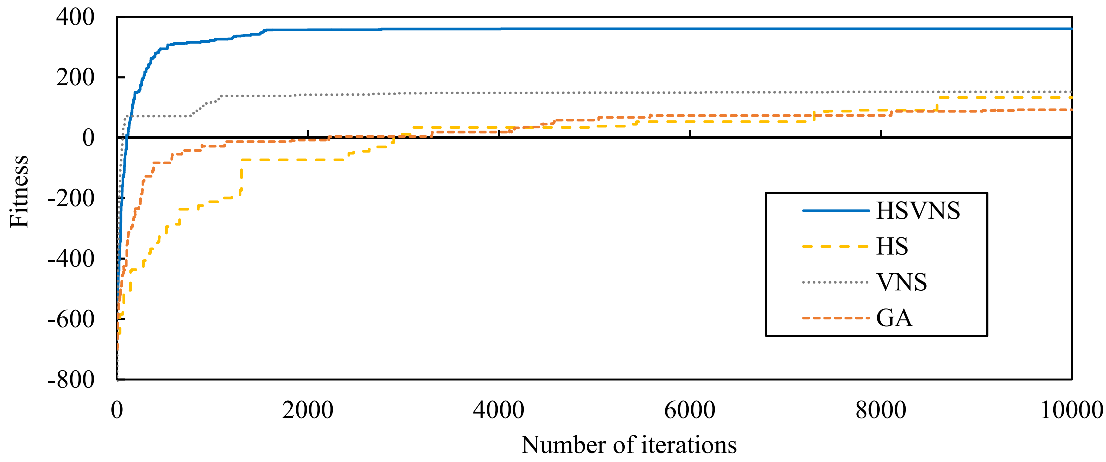

Figure 8. Convergence analysis of four algorithms.

5.2 Stability analysis

After a lot of trials, all the four algorithms must converge within 11 seconds. Hence, this subsection considers that each of the concerned four algorithms stops when the CPU time achieves 11 seconds. Then, the box plots for the experimental results of executing 20 times of the four algorithms are shown in Figure 9, and the statistics of these experimental results are shown in Table 2. From these results, on the average, the proposed HSVNS obtains the best fitness, and is the most stable (i.e., having the smallest standard deviation among the four algorithms). As for the average fitness, the VNS performs better than the HS. Hence, it is speculated that the VNS contributes more than the HS when using the proposed HSVNS to solve the concerned problem. Finally, the GA performs worst in all statistical measures. It is speculated that the GA is not suitable for solving the concerned problem because it may generate more infeasible solution during the crossover operation so that the solution repairing scheme causes solutions with much difference from the original solutions.

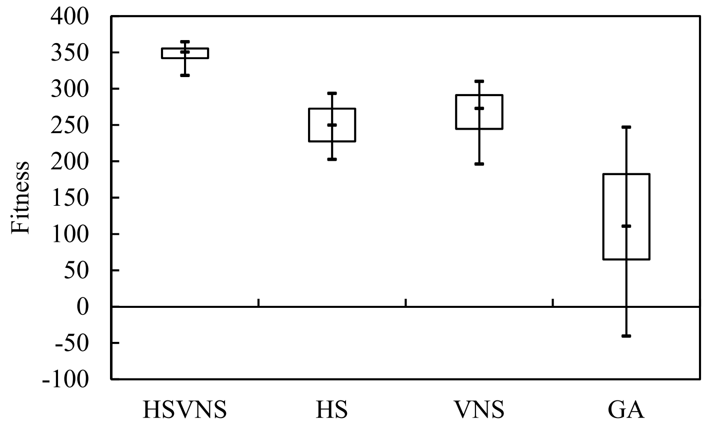

Figure 9. Box plots for the experimental results of executing 20 times of the four algorithms.

Table 2. Statistics of the simulation results of executing 20 times of four algorithms.

Method	Best fitness	Average fitness	Worst fitness	StdDev of fitness
HSVNS	370.50	350.35	324.73	11.25
HS	298.88	234.69	178.06	42.14
VNS	311.57	246.17	-42040	78.23
GA	267.92	72.59	-172.82	111.79

5.3 Analysis on harvesting different amounts of renewable energy

Consider Figure 4 to be the base case for the amount of the renewable energy harvested by the solar panel and the wind turbine. Then, Figure 10 shows the experimental analysis of executing the proposed HSVNS on 21 cases of obtaining different ratios (i.e., 0%, 10%, 20%, …, 200%) of the solar and wind energy amounts of the base case, respectively, while the other parameter settings remain unchanged. Note that the cases for harvesting less solar energy or wind energy amount (i.e., the cases of 0%, 10%, …, 90%) can be regarded as the cases at different degrees of bad weather conditions, bad solar irradiations, long night conditions, or other harsh environments where the renewable energy is not sufficient to be harvested. On the contrary, the cases of harvesting more solar or wind energy amount (i.e., those of 110%, 120%, …, 200%) can be regarded as the cases at different degrees of better harvest conditions than the base case.

From Figure 10, the proposed HSVNS in all cases can obtain fitness greater than 300. The best case (i.e., the fitness in the case with 200% of the solar energy amount of the base case is 501.34) obtains fitness about 35% higher than the base case. The worst case (i.e., the fitness in the case with no wind energy is 296.08) obtains fitness about 20% lower than the base case, but it still shows high effectiveness of the proposed HSVNS. When the renewable energy amount harvested does not charge a lot as compared to the base case (i.e., the cases of harvesting renewable energy amount between 70% and 130% of the base case), the proposed HSVNS obtains fitness within the range [350, 450].

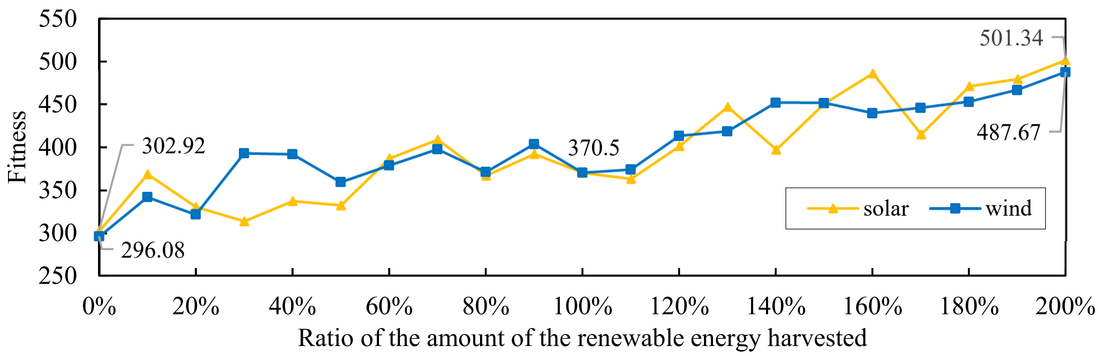

Figure 10. The experimental analysis of executing the proposed HSVNS when obtaining different ratios (i.e., 0%, 10%, 20%, …, 200%) of the solar and wind energy amounts of the base case, respectively.

5.4 *Analysis on using different adjustments*

Recall that the proposed HSVNS randomly selects two options to adjust solutions (i.e., Lines 7–13 in Algorithm 9). To analyze which adjustment option is better in solving the concerned problem, this subsection considers three algorithm settings: the HSVNS (i.e., with 50% to select either of the two options), the HSVNS with only the first option (i.e., Lines 8 – 9 in Algorithm 9), and the HSVNS with only the second option (i.e., Lines 11 – 13 in Algorithm 9). The box plots of executing 20 times of the three algorithm settings are shown in Figure 11, and the related statistics are shown in Table 3. From these results, if both options are adopted, the fitness has a remarkably better performance. For CPU time, there is no remarkable difference among three settings.

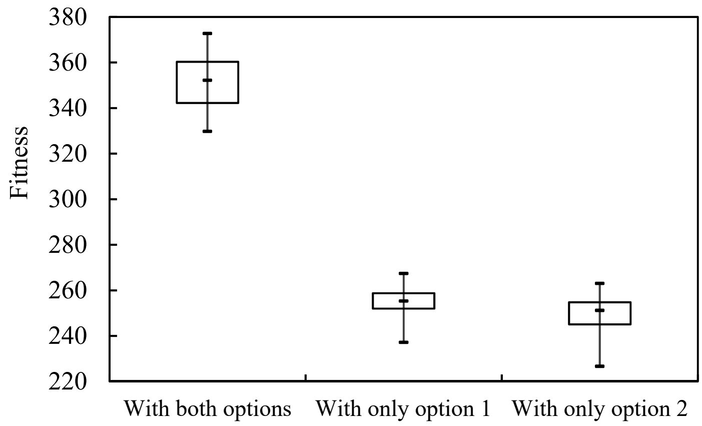

Figure 11. Box plots of running 20 times of the proposed HSVNS in three cases of using two adjustment options.

Table 3. Statistics of the experimental results of the HSVNS under different settings.

HSVNS setting	Best fitness	Average fitness	Worst fitness	StdDev of fitness	Average runtime (s)
With both options	370.50	350.35	324.71	11.25	14.22
With only option 1	268.25	255.48	233.12	7.47	15.35
With only option 2	265.81	250.65	236.19	8.33	13.33

5.5 Analysis on the amount of saving energy per house

This section analyzes the amount of saving the energy consumption from the electrical grid in each house in the experimental result for the problem instance with 5 houses. Figure 12 shows the energy consumption amount of each house for one day from the electrical grid in (a) the case without energy trading (i.e., Figure 7) and (b) the result generated by the HSVNS. The peak load (i.e., 57.6 kW) in Figure 12(a) occurs at hour 20; whereas the peak load (i.e., 15.9kW) in Figure 12(b) occurs at hour 19. That is, the peak load decreases by 41.7 kW, implying that the HSVNS has the capability of shifting the peak load. Furthermore, from the viewpoint of individual houses, each house decreases energy consumption from the electrical grid per day by 50kW, and the whole complex of houses saves energy consumption of 748.17kW. In addition, some houses do not consume any energy from the electrical grid for some hours (see Figure 12(b)).

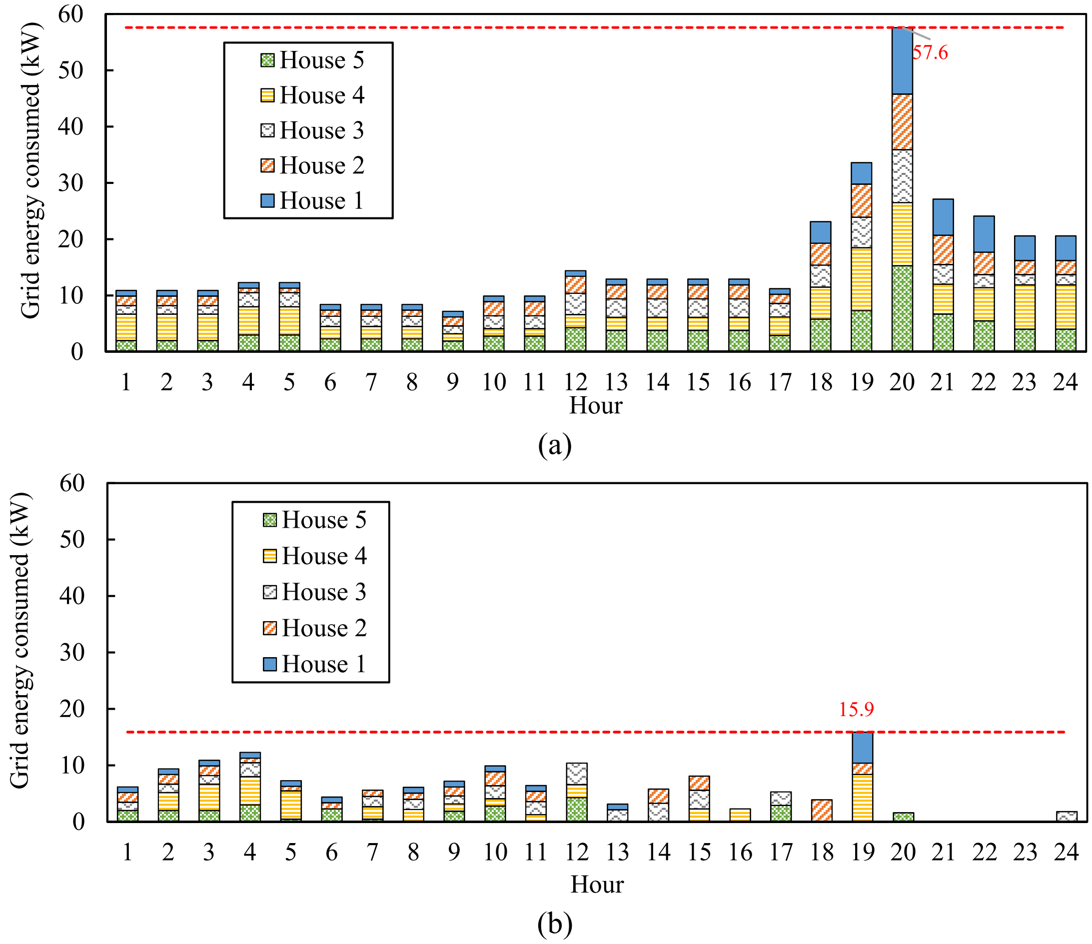

Figure 12. The energy amount consumed by each house for one day from the electrical grid in (a) the case without energy trading and (b) the result generated by the HSVNS.

5.6 Analysis on different numbers of houses in a complex

Consider the problem instances of small-scale complexes (with 5, 10, 15, …, and 50 houses), middle-scale complexes (with 75 and 100 houses), and large-scale complexes (with 125 and 150 houses). The average profit per house in the results of executing 5 times of the HSVNS on different-scale instances (under their respective best parameter settings) are shown in Figure 13. For each complex scale, the HSVNS can obtain profitable solutions for all problem instances, in which each house can earn a profit of at least 70¢ per day. Generally, the results for small-scale complexes have higher profit per house, in which the best profit (i.e., 107.45¢/day) is obtained in the case with 35 houses. After this case, the average profit per house decays with the increase of the number of houses. Note that more profitable solutions for the cases with large-scale complexes could be obtained, if the HSVNS is executed on a more efficient computing equipment.

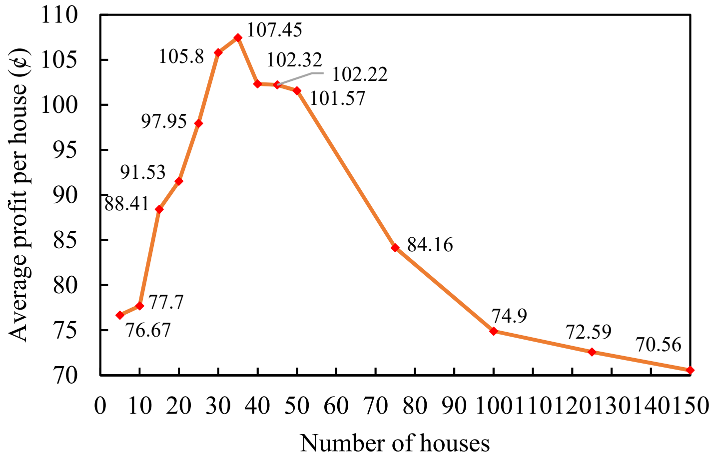

Figure 13. The average profit per house for one day in the results of executing 5 times of the HSVNS on different-scale problems.

6 Discussion

Although some previous works have investigated how to adjust the timing of charging/discharging ESSs to address the peak load shifting problem of the electrical grid, they rarely integrated the concept of sharing economy into the energy trading platforms for a complex of houses. Each house in the complex plays the role of a supplier and a demander at the same time, so that the whole complex is profitable under the IoE framework. The mathematical model of the concerned problem considers the revenue of storing energy in

BESSs (Constraints (4)), the operations of the energy trading platform (Constraints (11)–(12)), the decision variables of all patterns of energy flows (Constraints (13)–(55)), and the energy amount of each energy flow (Constraints (56)–(61)). The design of the proposed HSVNS algorithm integrates the features of two metaheuristic algorithms HS and VNS, and the simulation results show that the proposed HSVNS algorithm performs better than the classical HS, VNS, and GA in terms of convergence efficiency and fitness.

The differences of the proposed problem model from the previous models (e.g., [24]) are as follows:

- This model additionally considers the remaining value of the energy stored in the BESS (Constraint (5)).
- This model is the first to consider the energy sharing model of a complex of houses through an IoE with an energy trading platform, and hence the constraints for calculating the energy amount on the energy trading platform (Constraints (11)–(12)) are different from previous works.
- Different from previous works, this paper adopts binary decision variables for six energy flows of each house (Constraints (13)–(55)), and hence has different constraints for the energy amounts for the six energy flows (Constraints (56)–(61)).

As the green energy has received increasing attention, the ESS will become necessity in each house in the future. Although this paper considers adopting BESSs to store energy, the proposed problem and algorithm can be extended to adopting various types of ESSs (e.g, supercapacitor and flywheel). Other different problems on various types of ESSs have been investigated. For instance, Döşoğlu *et al.* [47] adopted active-passive compensatorssupercapacitor modeling and rotor EMF to improve low-voltage ride-through capability, so that the system can become stable in a short time. Adhikari *et al.* [48] proposed two indices to conduct the recovery-risk-analysis on the operating risk of wind power systems, and showed that it is more reliable to adopt fast-responding flywheel energy storage systems. Ramli *et al.* [49] adopted the PV/diesel hybrid system with flywheel energy storage to store redundant energy, and analyzed that deployment of this system can reduce fuel consumption and carbon emissions. Thus, a line of the future work is to consider diversified energy storage facilities and improve its performance (e.g., the optimal size and the charging efficiency of BESSs, stability of transmitting renewable energy, and how to provide stable energy sources when the renewable energy is not sufficient), and to include environmental concerns (e.g., mitigating the pollution from consuming the energy from electrical grids, and integrating the government policies on green energy). In addition, it would be of interest to improve the operating model of the energy trading platform (e.g., integrating the blockchain technology, so that houses can trade energy through smart contracts) and consider practical issues when implementing the platform.

7 Conclusion

This paper has constructed an MIP problem model for a complex of houses to share energy through the IoE with an energy trading platform so as to maximize the total profit of the whole complex of houses, and further proposed an HSVNS with a solution repairing scheme to solve this problem. Because the proposed problem model only considered the energy storage capacity of BESSs, it can be extended to being used in diversified types of

EESs. To evaluate performance of the proposed algorithm, the simulation was conducted on problems with complexes with 5 to 150 houses. Through simulation, the experimental results showed that the proposed HSVNS outperformed the classical HS, VNS, and GA in terms of convergence, stability, and fitness results. In addition, considering the base case with normal amounts of the renewable energy harvested in which the proposed HSVNS obtained fitness of about 370, this paper conducted experimental analysis of executing the proposed HSVNS on obtaining various renewable energy amounts of the base case. The results showed that when the harvested renewable energy amount fell between 70% and 130% of the base case, the proposed HSVNS obtained fitness within the range [350, 450]. From the simulation results on 5 houses, on the average, each house in different-scale complexes can obtain profits (at least 70¢ per day) from energy sharing and trading. In addition, the peak load of the electrical grid for one day decreased from 57.6 kW to 15.9 kW. From the aspect of the whole complex of houses, the energy consumption of 748.17kW can be saved. The energy consumption among houses in the complex has complementarity, i.e., each house can satisfy its energy demand during some time periods without buying energy from the grid, and even erns profits.

Although the simulation has shown that the proposed HSVNS performs well in shifting peak loads in one day of the spring and winter seasons, the real-world situation has a variety of changes, including change of weather conditions, long night conditions, and change of solar irradiation. Hence, a potential line of future work is to consider real data in simulation. In addition, it would be interesting to incorporate the proposed energy trading platform with different industries to create new business models. On the other hand, the simulation in this paper is conducted for only one day, and hence it is also of future interest to conduct simulation for a longer time period.

Acknowledgements

This work has been supported in part by the Ministry of Science and Technology, Taiwan, under Grants MOST 109-2221-E-009-068-MY3 and MOST 106-2221-E-009-101-MY3; and the Ministry of Education, Taiwan, under the Higher Education Sprout Project.

References

[1] Fang X, Misra S, Xue G, Yang D. Smart grid—The new and improved power grid: A survey. *IEEE Communications Surveys & Tutorials* 2012;14(4):944–980.

[2] Olabi AG, Onumaegbu C, Wilberforce T, Ramadan M, Abdelkareem MA, Al-Alami AH. Critical review of energy storage systems. *Energy* 2020;214:118987.

[3] Pfeifer A, Dobravec V, Pavlinek L, Krajačić G., Duić N. Integration of renewable energy and demand response technologies in interconnected energy systems. *Energy* 2018;161:447–455.

[4] Rahman S, Rinaldy. An efficient load model for analyzing demand side management impacts. *IEEE Transactions on Power Systems* 1993;8(3):1219–1226.

[5] Klein LP, Matos LM, Allegretti G, Silva MG. A pragmatic approach towards end-user engagement in the context of peer-to-peer energy sharing. *Energy* 2020;118001.

[6] Lin CC, Deng DJ, Liu WY, Chen L. Peak load shifting in the Internet of energy with energy trading among end-users. *IEEE Access* 2017;5:1967–1976.

[7] Lin CC, Deng DJ, Kuo CC, Liang YL. Optimal charging control of energy storage and electric vehicle of an individual in the Internet of energy with energy trading. *IEEE Transactions on Industrial Informatics* 2018;14(6):2570–2578.

[8] Uddin M, Romlie MF, Abdullah MF, Halim SA, Kwang TC. A review on peak load shaving strategies. *Renewable and Sustainable Energy Reviews* 2017;82(3):3323–3332.

[9] Xu F, Chen X, Zhang M, Zhou Y, Wang Y. A sharing economy market system for private EV parking with consideration of demand side management. *Energy* 2020;190:116321.

[10] Lijesen MG. The real-time price elasticity of electricity. *Energy Economics* 2007;29(2):249–258.

[11] Qian LP, Zhang YJA, Huang J. Demand response management via real-time electricity price control in smart grids. *IEEE Journal on Selected Areas in Communications* 2013;31(7):1268–1280.

[12] Yoon JH, Baldick R, Novoselac A. Dynamic demand response controller based on real-time retail price for residential buildings. *IEEE Transaction on Smart Grid* 2014;5(1):121–129.

[13] Duggirala VA, Gundavarapu VNK. Improved LVRT for grid connected DFIG using enhanced field oriented control technique with super capacitor as external energy storage system. *Engineering Science and Technology, an International Journal* 2016;19(4):1742–1752.

[14] Döşoğlu MK, Arsoy AB, Güvenç U. Application of STATCOM-supercapacitor for low-voltage ride-through capability in DFIG-based wind farm. *Neural Computing and Applications* 2017;28(9):2665–2674.

[15] Döşoğlu MK., Arsoy AB. Transient modeling and analysis of a DFIG based wind farm with supercapacitor energy storage. *International Journal of Electrical Power & Energy Systems* 2016;78:414–421.

[16] Döşoğlu MK. Nonlinear dynamic modeling for fault ride-through capability of DFIG-based wind farm. *Nonlinear Dynamics* 2017;89(4):2683–2694.

[17] Mishra Y, Mishra S, Li F. Coordinated tuning of DFIG-based wind turbines and batteries using bacteria foraging technique for maintaining constant grid power output. *IEEE Systems Journal* 2011;6(1):16–26.

[18] Abdeltawab HH, Mohamed YARI. Robust energy management of a hybrid wind and flywheel energy storage system considering flywheel power losses minimization and grid-code constraints. *IEEE Transactions on Industrial Electronics* 2016;63(7):4242–4254.

[19] Hamzaoui I, Bouchafaa F, Talha A. Advanced control for wind energy conversion systems with flywheel storage dedicated to improving the quality of energy. *International Journal of Hydrogen Energy* 2016;41(45):20832–20846.

[20] Song Z, Hou J, Xu S, Ouyang M, Li J. The influence of driving cycle characteristics on the integrated optimization of hybrid energy storage system for electric city buses. *Energy* 2017;135:91–100.

[21] Reihani E, Sepasi S, Roose LR. Energy management at the distribution grid using a battery energy storage system (BESS). *International Journal of Electrical Power & Energy Systems* 2016;77:337–344.

[22] Teleke S, Baran ME, Anderson L. Control strategies for battery energy storage for wind farm dispatching. *IEEE Transactions on Energy Conversion* 2009;24(3):725–732.

[23] Lawder MT, Suthar B, Northrop PW. Battery energy storage system (BESS) and battery management system (BMS) for grid-scale applications. *Proceedings of the IEEE* 2014;102(6):1014–1030.

[24] Ospina J, Gupta N, Newaz A, Lofman G. Sampling-based model predictive control of PV-integrated energy storage system considering power generation forecast and real-time price. *IEEE Power and Energy Technology Systems Journal* 2019;6(4):195–207.

[25] Yi P, Zhu T, Jiang R, Wang B. Deploying energy routers in an energy internet based on electric vehicles. *IEEE Transactions on Vehicular Technology* 2016;65(6):4714–4725.

[26] Mahmud K, Town GE, Morsalin S. Integration of electric vehicles and management in the Internet of energy. *Renewable and Sustainable Energy Reviews* 2018;82:4179–4203.

[27] Moghaddam MHY, Leon-Garcia A. A fog-based Internet of energy architecture for transactive energy management systems. *IEEE Internet of Things Journal* 2018;5(2):1055–1069.

[28] Lv Z, Kong W, Zhang X, Lu X. Intelligent security planning for regional distributed energy Internet. *IEEE Transactions on Industrial Informatics* 2019;16(5):3540–3547.

[29] Mahmud K, Khan B, Siano P. An Internet of energy framework with distributed energy resources, prosumers and small-scale virtual power plants: An overview. *Renewable and Sustainable Energy Reviews* 2020;127:109840.

[30] Alvaro-Hermana R, Fraile-Ardanuy J, Zufiria PJ. Peer to peer energy trading with electric vehicles. *IEEE Intelligent Transportation Systems Magazine* 2016;8(3):33–44.

[31] Vahedipour-Dahraie M, Rashidizadeh-Kermani H, Siano P. Peer-to-peer energy trading between wind power producer and demand response aggregators for scheduling joint energy and reserve. *IEEE Systems Journal* 2020; in press.

[32] Zhang C, Wu J, Zhou Y, Cheng M. Peer-to-peer energy trading in a microgrid. *Applied Energy* 2018;220:1–12.

[33] Wang Y, Wang X, Shao C, Gong N. Distributed energy trading for an integrated energy system and electric vehicle charging stations: A Nash bargaining game. *Renewable Energy* 2020;155:513–530.

[34] Zhang W, Wei W, Chen L, Zheng B, Mei S. Service pricing and load dispatch of residential shared energy storage unit. *Energy* 2020;117543.

[35] Cui S, Wang YW, Li C, Xiao JW. Prosumer community: A risk aversion energy sharing model. *IEEE Transactions on Sustainable Energy* 2019;11(2):828–838.

[36] Huang P, Lovati M, Bales C. A coordinated control to improve performance for a building cluster with energy storage, electric vehicles, and energy sharing considered. *Applied Energy* 2020;268:114983.

[37] Geem ZW, Kim JH, Loganathan GV. A new heuristic optimization algorithm: Harmony search. *Simulation* 2001;76(2):60–68.

[38] Rao RS, Narasimham SVL, Raju MR, Rao AS. Optimal network reconfiguration of large-scale distribution system using harmony search algorithm. *IEEE Transactions on Power Systems* 2010;26(3):1080–1088.

[39] Elattar EE. Modified harmony search algorithm for combined economic emission dispatch of microgrid incorporating renewable sources. *Energy* 2018;159:496–507.

[40] Nazari-Heris M, Babaei AF, Mohammadi-Ivatloo B, Asadi S. Improved harmony search algorithm for the solution of non-linear non-convex short-term hydrothermal scheduling. *Energy* 2018;151:226–237.

[41] Todosijević R, Mladenović M, Hanafi S, Mladenović N, Crévits I. Adaptive general variable neighborhood search heuristics for solving the unit commitment problem. *International Journal of Electrical Power & Energy Systems* 2016;78:873–883.

[42] Mladenović N, Hansen P. An introduction to variable neighborhood search. In: Voß S, et al., editors. *Meta-heuristics*, Boston, MA: Springer; 1999, p. 433–458.

[43] Roberts B, Sandberg C. The role of energy storage in development of smart grids. *Proceedings of the IEEE* 2011;99(6):1139–1144.

[44] Taiwan Power Company, Renewable energy, available at: https://pro.re.org.tw/use.aspx, accessed in Feb., 2019.

[45] Commonwealth Edison Company. Real-time hourly prices, https://hourlypricing.comed.com/live-prices/; 2019 [accessed August 2019].

[46] Tutkun N, Can Ö, Şan ES. Daily cost minimization for an off-grid renewable microhybrid system installed to a residential home. In: *ICRERA 2015: Proceedings of 4th International Conference on Renewable Energy Research and Applications*; 2015 Nov 22-25; IEEE Press; 2015. p. 750–754.

[47] Döşoğlu MK, Özkaraca O, Güvenç U. Novel active-passive compensator-supercapacitor modeling for low-voltage ride-through capability in DFIG-based wind turbines. *Electrical Engineering* 2019;101(4):1119–1132.

[48] Adhikari S, Karki R, Piya, P. Recovery risk mitigation of wind integrated bulk power system with flywheel energy storage. *IEEE Transactions on Power Systems* 2019;34(5):3484–3493.

[49] Ramli MA, Hiendro A, Twaha S. Economic analysis of PV/diesel hybrid system with flywheel energy storage. *Renewable Energy* 2015;78: 398–405.